Open Veterinary Journal, (2015), Vol. 5(2): 173-178
ISSN: 2226-4485 (Print)
ISSN: 2218-6050 (Online)

Case Report

Submitted: 02/09/2015 Accepted: 23/11/2015 Published: 22/12/2015

Ultrasound and multidetector computed tomography of mandibular salivary gland adenocarcinoma in two dogs

D. Lenoci[1] and M. Ricciardi[2,*]
[1]*Private Practitioner, Bari, Italy*
[2]*"Pingry" Veterinary Hospital, via Medaglie d'Oro 5, Bari, Italy*

Abstract
Malignant tumors of the salivary glands are rare in dogs, with adenocarcinoma being the most represented. Parotid and mandibular glands are most commonly affected in dogs. Because of local invasivity and high metastatic potential, preoperative imaging evaluation of mandibular region and tumoral staging is essential along with biopsy sampling. The present manuscript describes the ultrasound and computed tomographic imaging findings of mandibular gland adenocarcinoma in two dogs and discusses their clinical utility.
Keywords: Computed tomography, Dog, Salivary gland tumor, Ultrasound.

Introduction

The major causes of localized bulging in the upper neck region in dogs include salivary mucoceles, sialoadenitis, sialolithiasis, lymph nodes abscesses, salivary gland infarction and foreign bodies, lymph node and salivary gland tumours (Militerno *et al*., 2005; Torad and Hassan, 2013). Salivary gland neoplasms are described as rare accounting for 0.17% of all small animal tumors (Carberry *et al*., 1988). In dogs mandibular and parotid glands seem to be most commonly involved without breed and sex predisposition (Spangler and Culbertson, 1991; Hammer *et al*., 2001; Marconato and Amadori 2012). Among malignant salivary gland tumors several histotypes have been reported with adenocarcinoma being the most represented (Head and Else, 2002; Head *et al*., 2003; Sozmen *et al*., 2003).

These neoplasms are considered extremely aggressive, usually locally invasive, so they may extend through the capsule of the gland to infiltrate adjacent tissues; rapid metastatization to regional lymph nodes and to other organs, such as lungs and bones, is also described in the progression of the disease (Burek *et al*., 1994; Habin and Else, 1995; Morris and Dobson, 2001). As for all localized tumors the treatment of choice is the surgical removal with a surgical success rate depending on the local invasivity and involvement of surrounding vital structures. Adjunctive radiation therapy or chemotherapy may be considered following surgery (Evans and Thrall, 1983). Median survival times in most aggressively treated cases is 1 - 2 years (Hammer *et al*., 2001). Furthermore, literature indicates that early diagnosis significantly improves the survival times in dogs (Hammer *et al*., 2001; Sidaway *et al*., 2004).

To date different reports have described the clinical approach for mandibular gland malignancies in dogs, underlying the importance of cytopathological and histopathological evaluation before and after surgical treatment (Militerno *et al*., 2005; Smrkovski *et al*., 2006; Almeida *et al*., 2010). In this scenario specific veterinary literature regarding the imaging appearance of these neoplasms on ultrasound and CT examinations is scarce with only sporadic descriptions and images available for review (Smrkovski *et al*., 2006; Marconato and Amadori, 2012;). This paper describes and compares the ultrasonographic and computed tomography imaging findings in two cases of canine mandibular gland adenocarcinoma and discusses the role of these two techniques in the diagnostic utility of this disease.

Case Details

Dog 1

An 11-year-old intact male dalmatian dog was evaluated for a 2-months history of progressive left submandibular swelling. On physical examination the patient did not show any abnormality except for a fixed, firm non-painful subcutaneous mass located ventro-caudal to the left mandibular angle. No mandibular lymph nodes enlargement was evident on palpation. Hematobiochemical and urinalysis were normal.

Dog 2

A 13-year-old intact female dalmatian dog was evaluated for a bulky swelling in the right mandibular region first noted by the owner 30 days before. At palpation the mass appeared soft, non-painful and slightly mobile with respect to surrounding tissue. Because of the considerable dimensions of the mass the evaluation of mandibular lymph nodes was difficult. General physical examination, hematobiochemical and urinalysis were normal.

***Corresponding Author:** Mario Ricciardi. "Pingry" Veterinary Hospital, via Medaglie d'Oro 5, Bari, Italy.
E-mail: ricciardi.mario@alice.it

Imaging

Dog 1

In order to clarify the anatomical origin of the neoformation, a B-mode ultrasound examination of the upper neck was performed with the dog in dorsal recumbency, using a portable ultrasound machine (MyLab 30 Gold Vet®, Esaote, Genoa, Italy), with a linear, high frequency, transducer 10–18 MHz. Ultrasound videotapes and static images were reviewed. Presence of the following ultrasonographic abnormalities were recorded: Left submandibular gland enlargement with increased sphericity index, well-circumscribed, hypoechoic, inhomogeneous parenchymal echogenicity with several small mineral foci and tortuous vessels (Fig. 1). These findings were suggestive of primary mandibular gland neoplasia. Differential diagnoses included sialoadenitis, but it was considered less likely due to the presence of parenchymal mineralizations.

Based on the suspicious of primary neoplasm, multidetector computed tomography of the whole body was performed immediately after the ultrasound examination for regional anatomical characterization and complete staging. A 16-slice MDCT scanner (Somatom Emotion, Siemens, Forchheim, Germany) was used with the patient in sternal recumbency on the CT table under general anesthesia. Computed tomography images were acquired before and after the intravenous injection of iodinate contrast medium (640 mg I/kg; *Iopamigita® Insight Agents GmbHR, Heildeberg, Germany*) using the following technical parameters: Standard acquisition algorithm, 110 kVp, 200 mAs, 1.5-mm slice thickness, pitch of 0.8, and 0.6 s/rotation. Three-dimensional (3D) multiplanar reformatted images were obtained using a dedicated 3D software (Pixmeo, OsiriX; OsiriX DICOM-viewer; Pixmeo, Geneva, Switzerland). Computed tomography scans showed enlargement of the left mandibular salivary gland. The abnormal parenchima appeared homogeneous, isoattenuating to the soft tissue, with multiple irregular areas hypoattenuating to the soft tissue mixed to small foci hyperattenuating to the soft tissue suggestive of mineralizations. No enlargment of ipsilateral mandibular lymph nodes were seen while the left medial retropharingeal lymph node was enlarged compared to the controlateral one. No vascular or parotid compressions were evident. No muscular infiltrations were seen (Fig. 2).

Dog 2

Diagnostic work-up continued with regional ultrasound and total-body computed tomography as described for dog 1.

Ultrasound evaluation revealed a large heterogeneous cavitated mass in the soft tissues of the neck, on the right side. The marginal parenchyma was hypoecoic with mineral foci while the central component

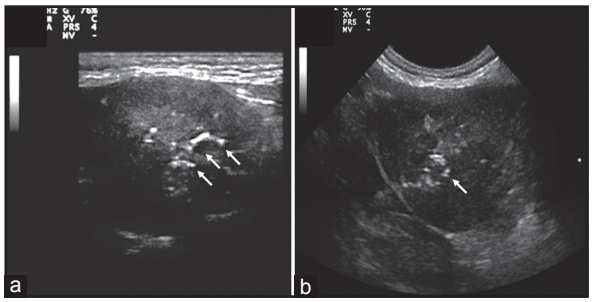

Fig. 1. Dog 1. Longitudinal (a) and transversal (b) ultrasound scans of the left submandibular gland - ventral approach. There is enlargement of the gland with a hinomogeneous, hypo echoic parenchyma and small hyperechoic calcific foci (arrows).

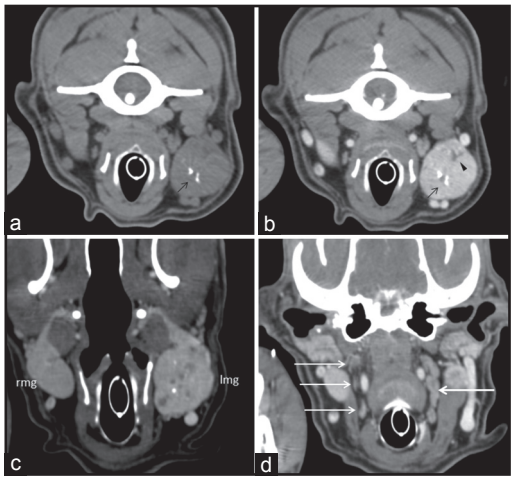

Fig. 2. Dog 1. Unenhanced (a) and contrast-enhanced (b) transverse comptuted tomography images of the neoplastic left mandibular gland. Oblique Dorsal multiplanar reformatted CT images at level of mandibular glands (c) and medial retropharyngeal lymphnodes (d). The affected gland appeared enlarged compared to the contralateral one (c) with parenchimal mineralizations (black arrows) and small hypoattenuating areas suggestive of necrosis (b, arrowhead). The left medial retropharyngeal lymph node (b, single arrow) was enlarged compared with its contralateral (d, triple arrows). Rmg: right mandibular gland; lmg: left mandibular gland.

appeared anechoic with irregular contours and far enhancement, suggestive of free fluid. The mass was suspected to originate from thyroid gland, but after ultrasound-guided drainage of the fluid component, the empty mass appeared caudal to the more hypoecocic digastricus muscle, landmark of mandibular salivary glands (Fig. 3). The medial retropharingeal lymph node was hypoecoic and enlarged.

CT showed significant enlargement of the right mandibular salivary gland. This structure appeared on native images as a large fluid-filled cavity hypoattenuating to the soft tissue (mean attenuation

value: 25 HU) surrounded by irregular peripheral tissue and crossed by multiple septa isoattenuating to the soft tissue. Multiple small irregular foci hyperattenuating to the soft tissue (mean attenuation value: 278 HU)

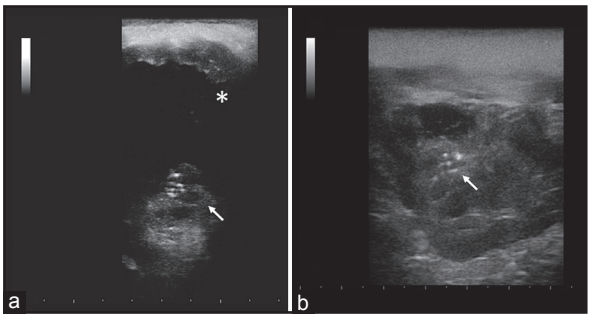

Fig. 3. Dog 2. Transverse ultrasound scans of the right submandibular gland, before (a) and after (b) ultrasound guided drainage - ventral approach. The gland is enlarged with anhecoic fluid filled cavity (a, asterisk). The solid component shows heterogeneous echogenicity with small hyperechoic calcific foci (arrows). Residual intraparenchimal fluid (asterisk) and calcific foci (arrow) are seen after drainage of the fluid component (b).

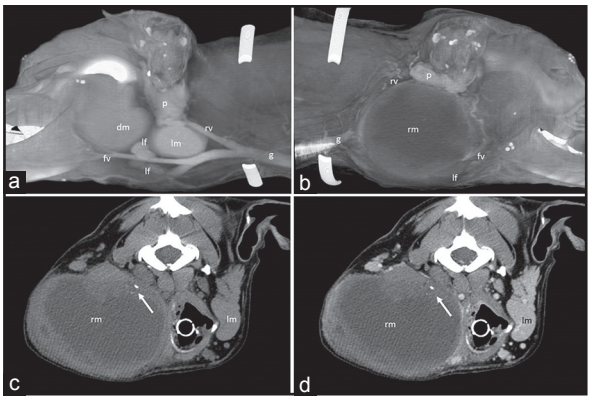

Fig. 4. Dog 2. Volume rendered computed tomography images of the left (a) and right (b) mandibular region. Unenhanced (c) and contrast-enhanced (d) transverse comptuted tomography images of the neoplastic right mandibular gland. The affected gland (rm) appeared as a cavitated mass with omogeneous hypoattenuating fluid content and focal mineralization (arrows). The enhancement of peripheral parenchymal component was poor. Volume rendered image of the right mandibular region (b) clarified the relationships between the neoplastic gland and surrounding structures especially if compared with the normal anatomy of the left side (a). The mass displaced dorsally the parotid gland (p) and compressed the retromandibular vein (rv), facial vein (fv) and mandibular lymph nodes (lf). No sign of muscular or bone infiltration were evident. (g) jugular vein; lm: left mandibular gland; dm: digastric muscle.

suggestive of mineralizations were seen within the parenchymatous component of the mass. No significant enhancement of the neoformation was noted after intravenous contrast medium administration (Fig. 4). Right mandibular and medial retropharingeal lymph nodes enlargement was associated. The linguofacial and maxillary veins were not visible immediately cranial to the bifurcation of the external jugular vein where they came in close connection to the mass. These findings were suggestive of vascular compression. The right parotid gland appeared also compressed between the mass and the ear canal. No muscular infiltrations were seen. Within the left lung multiple homogeneous nodular lesions isoattenuating to the soft tissue were seen diffuse in the cranial and caudal lobes (Fig. 5).

Based on ultrasound and CT findings a presumptive diagnosis of primary neoplasia of the left (dog 1) and right (dog 2) mandibular glands was made in both patients. Sialoadenitis in dog one was considered less likely. In both dogs regional lymph nodes appeared involved and in dog 2 the nodular lesions within the left lung appeared compatible with pulmonary metastasis.

Outcome

Dog 1 underwent surgical excision of the pathologic mandibular glands and retropharyngeal lymph node. In dog 2 a bioptic sample of the neoformation was taken but complete surgical excision was refused by the owner. All the removed tissues were then submitted for histopathology.

In both dogs the histopathologic examination revealed glandular tissue infiltrated by a non-encapsulated

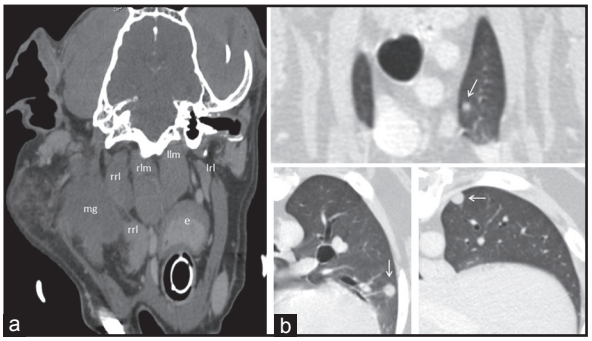

Fig. 5. Dog 2. (a) Oblique dorsal multiplanar reformatted contrast-enhanced CT image at level of medial retropharyngeal lymph nodes. Transverse contrast-enhanced CT image at the level of cranial lobe (b), middle part (c) and caudal lobe of the left lung. Right medial retropharyngeal lymph node (rrl) was enlarged compared to its contralateral (lrl). In different parts of the left lung multiple round nodular lesions isoattenuating to soft tissue, were present, compatible with pulmonary metastasis. mg: right mandibular gland – dorsal margin; rlm: right longus capitis muscle; llm: left longus capitis muscle; e: esophagus.

neoplastic proliferation. Neoplastic tissue consisted of tubules and clusters of pleomorphic epithelial cells with moderate-high nuclear-cytoplasmic ratio, round or oval central nucleus, vesicular chromatin and one or more nucleoli. A thick, dense fibrous stroma with centers of cartilaginous metaplasia sustained the neoplastic tissue. In different points the cells were arranged around necrotic centers. Mitotic rate ranged from one to four mitosis per high-power field. In dog 2 the immunohistochemical staining of neoplastic cells demonstrated intense cytoplasmatic expression of cytokeratin. These findings were suggestive of salivary gland adenocarcinoma. In dog 1 histopathologic evaluation of the medial retropharyngeal lymph node revealed a reactive hyperplasia without signs of neoplastic infiltration.

In dog 1 no local complications were observed soon after tumor removal. After surgery, the dog was treated with enrofloxacin (5 mg/kg daily per os) for a week. Two days after surgery the dog started to eat autonomously and 90 days later no recurrence of the disease was noted. Monitoring of the mandibular region and lungs was recommended to the owner.

Surgery and chemotherapy were both refused by the owner of dog 2.

Discussion

In human medical literature imaging is always included in the diagnostic setting of patients with salivary gland tumor before cytopatologic sampling or in conditions where there are some limitations in performing fine needle aspiration (FNA), such as unusual location or patients' unwillingness (Liu *et al*., 2015). Besides identifying the masses of salivary glands, imaging is also useful in differentiating them from the masses/pathologies of adjacent cervical spaces. Nodal masses, peripheral nerve schwannomas, and masseteric hypertrophy may mimic tumors of salivary glands clinically. In proven cases of salivary gland tumors, imaging helps in delineating the extent of the lesion and invasion of adjacent cervical spaces, skull base, mandible, and nerves/meninges (Welkoborsky, 2011; Rastogi *et al*., 2012; Carotti *et al*., 2014;).

Because of their superficial anatomic location, distinct borders and homogenous echotexture, the salivary glands are ideally positioned for sonographic assessment. The advantages of this technique include high diagnostic accuracy, non-invasiveness, lack of radiation exposure, high reproducibility, low costs and possibility of ultrasound-guided fine-needle biopsy (Welkoborsky, 2011). When combined with color Doppler imaging, ultrasound (US) helps in assessing the vascularity and nature of the lesion (malignant vs benign lesions) (Rastogi *et al*., 2012). In a previous study US achieved a sensitivity of 88%, a specificity of 54% in assessing a tumor entity-maligne or benigne (Rudack *et al*., 2007).

Ultrasound and CT have been already reported as useful diagnostic tools for the evaluation of different salivary gland pathologies in dogs such as sialolithiasis (Lee *et al*., 2014) mucocele (Torad and Hassan, 2013) and sialoadenitis (Cannon *et al*., 2011). In these reports ultrasound and computed tomography (CT) allowed a precise identification of the affected glands and a detailed morphologic evaluation of the type of disease. However, descriptions of imaging findings of salivary gland tumor in dogs are limited to a single reported case of pleomorphic adenoma of the mandibular gland in a Basset Hound in which computed tomography was performed (Smrkovski *et al*., 2006). To the authors' knowledge this is the first report describing and comparing the US and CT characteristics of salivary gland adenocarcinomas in dogs, evaluating the clinical utility of these imaging techniques for the diagnosis of this disease.

In our cases ultrasound examination alone was sufficient to identify the tumors, appearing as a first-line tool for the imaging diagnosis of salivary neoplastic pathology. However, in cases of very large masses, as seen in dog 2, ultrasound could not accurately identify their anatomical location and define possible infiltrations of surrounding soft tissue.

In human medicine, CT and MRI are commonly used as adjunctive imaging diagnostic methods for salivary gland tumors, usually following US examination. CT, with its good anatomic resolution, soft tissue contrast, and morphologic detail, can provide meaningful information regarding deep located masses, bone invasion and may help the surgeons during the procedure (Liu *et al*., 2015).

Analysis of different enhancement patterns by using dynamic multidetector computed tomography (MDCT) demonstrated to be helpful in the differential diagnosis of salivary gland tumors and for distinction between adenomas and malignant tumors (Choi *et al*., 2000; Yerli *et al*., 2007).

In our cases CT scan confirmed the ultrasonographic findings related to the neoplastic salivary glands and provided useful adjunctive information on the relationships between the masses and adjacent musculature (evaluation of muscular infiltration or compression), jugular vein tributaries, especially in dog 2, regional lymph nodes involvement, particularly the deep medial retropharyngeal. Furthermore CT allowed complete whole body scan in few seconds for oncologic staging, according to the Tumor-Node-Metastasis (TNM) classification reported for salivary gland tumor in animals (Thackray and Sobin, 1972).

Accordingly to the report in human medical literature (Rudack *et al*., 2007), we did not find significant differences between US and CT for regional anatomic evaluation. Both US and CT appeared specific for identification of the affected glands with respect

to the surrounding parotid gland, mandibular and retropharyngeal lymph nodes and adjacent musculature. However, assessment of vascular displacement (maxillary and linguofacial veins) and pulmonary distant metastasis in dog 2 was clarified on CT images. Furthermore no difference in the appearance of tumoral parenchyma was evident comparing the US and CT findings. The pathologic gland tissue varied in these two dogs from hynomogeneous solid mass with focal mineralization and fluid areas (suggestive of necrotic foci as then confirmed by histopathology) to large cystic-like mass with sporadic parenchymal mineralizations.

Calcifications and necrotic foci have been reported as imaging findings in carcinomatous changes of salivary glands both in humans and dogs (Marconato and Amadori, 2012; Li *et al*., 2014) and were clearly identified both on US and CT scans in the two cases we described.

Different from what is commonly described for salivary gland tumors (Habin and Else, 1995; Morris and Dobson, 2001; Militerno *et al*., 2005;) in this two dogs the growth pattern appeared purely expansive without infiltrations of surrounding structures even taking into account the big dimensions reached by neoplastic gland in dog 2.

Lymphatic drainage of the mandibular gland is pertaining to the medial retropharyngeal lymph node (Evans and de Lahunta, 2013). Ipsilateral mandibular lymph nodes were enlarged in dog 2 while in both dogs an ipsilateral medial retropharingeal lymphadenopathy was evident in both US and CT images. Differently from mandibular lymph nodes that are superficial and palpable, medial retropharingeal lymph nodes are deeply located in the neck, medially to the mandibular gland and just caudal to the proximal insertion of digastricus muscle (Evans and de Lahunta, 2013). This lymph nodes appeared easily evaluable on first US examination as previously described in dogs (Burns *et al*., 2008). In dog 1 the imaging finding of lymph node involvement was confirmed on histopathology as reactive lymphoadenopathy without signs of neoplastic involvement. Total-body CT staging in dog 2 revealed multiple nodular lesions within the left lung suggestive of distant metastasis. In a study on twenty-four dogs with salivary tumors 17% and 8% of patients had lymph node and distant metastasis, respectively (Hammer *et al*., 2001). In the authors' opinion, giving the high metastatic potential of the salivary gland adenocarcinoma towards regional lymph nodes and distant organs, regional evaluation, lymph nodes mapping and extensive whole-body scan are essential for tumoral staging, accordingly to the TNM classification (Thackray and Sobin, 1972), and can be helpful for an accurate surgical planning.

In conclusion, US and CT are reliable methods in diagnosing salivary gland tumors clinically in people (Rastogi *et al*., 2012), and findings from the present study supported the use of ultrasonography as a useful diagnostic tool for characterizing these disease in dogs before FNA or biopsy sampling and surgery. In both patients the overall imaging findings oriented toward a presumptive diagnosis of mandibular gland neoplasia. Salivary gland tissue could be differentiated from lymph node tissue and other neighboring structures based on sonographic characteristics. These findings support the use of US as first regional imaging for mandibular gland tumors characterization.

Even if significant differences between US and CT findings on mandibular gland were not detected in our patients, computed tomography revealed its clinical utility for peritumoral vascular assessment, medial retropharyngeal lymph nodes evaluation and total-body staging for detection of distant metastasis. Contrary to what was reported in human medical literature, preoperative assessment of salivary gland tumor is not routinely adopted in small animal practice based on the few veterinary reports on these disorders. To the author opinion regional and total-body imaging evaluation, with on US and CT respectively, are useful for the diagnostic, clinical and surgical management of mandibular gland adenocarcinoma in dogs.

Acknowledgments

The authors wish to thank all the staff of the Pingry Veterinary Hospital of Bari, Italy for their assistance with data collection.

Conflict of interest

The authors declare that there is no conflict of interest.

References

Almeida, A.P., Malm, C., Lavalle, G., Cassali, G.D., Santos, R.L. and Paixão, T.A. 2010. Salivary gland carcinosarcoma in a dog. Braz. J. Vet. Pathol. 3, 137-141.

Burek, D.A., Munn, R.J. and Madewell, B.R. 1994. Metastatic adenocarcinoma of a minor salivary gland in a cat. Zentralbl. Veterinarmed. A. 41, 485-490.

Burns, G.O., Scrivani, P.V., Thompson, M.S. and Erb, H.N. 2008. Relation between age, body weight, and medial retropharyngeal lymph node size in apparently healthy dogs. Vet. Radiol. Ultrasound 49, 277-281.

Cannon, M.S., Paglia, D., Zwingenberger, A.L., Boroffka, S.A., Hollingsworth, S.R. and Wisner, E.R. 2011. Clinical and diagnostic imaging findings in dogs with zygomatic sialadenitis: 11 cases (1990-2009). J. Am. Vet. Med. Assoc. 239, 1211-1218.

Carberry, C.A., Flanders, J.A., Harvey, H.J. and Ryan, A.M. 1988. Salivary gland tumors in dogs

and cats: A literature and case review. J. Am. Anim. Hosp. Assoc. 24, 561-567.

Carotti, M., Ciapetti, A., Jousse-Joulin, S. and Salaffi, F.U. 2014. Ultrasonography of the salivary glands: The role of grey-scale and colour/power Doppler. Clin. Exp. Rheumatol. 32, S61-70.

Choi, D.S., Na, D.G., Byun, H.S., Ko, Y.H., Kim, C.K., Cho, J.M. and Lee, H.K. 2000. Salivary gland tumors: Evaluation with two-phase helical CT. Radiology 214, 231-236.

Evans, E. and de Lahunta, A. 2013. Miller's anatomy of the dog, 4th ed. Philadelphia, PA: Elsevier.

Evans, S.M. and Thrall, D.E. 1983. Postoperative orthovoltage radiation therapy of parotid salivary gland adenocarcinoma in three dogs. J. Am. Vet. Med. Assoc. 182, 993-994.

Habin, D.J. and Else, R.W. 1995. Parotid salivary gland adenocarcinoma with bilateral ocular and osseous metastases in a dog. J. Sm. Anim. Pract. 36, 445-449.

Hammer, A., Getzy, D., Ogilvie, G., Upton, M., Klausner, J. and Kisseberth, W.C. 2001. Salivary gland neoplasia in the dog and cat: Survival times and prognostic factors. J. Am. Anim. Hosp. Assoc. 37, 478-482.

Head, K.W. and Else, R.W. 2002. Tumors of the skin and soft tissues. In: Tumors in domestic animals. DJ Meuten (ed.), 4th ed. Iowa State Press, Ames, IA. pp: 410-416.

Head, K.W., Cullen, J.M., Dubielzig, R.R., Else, R.W., Midsorp, W., Patnaik, A.K., Tateyama, S. and van der Gaag, I. 2003. Classification of Salivary gland tumors of Domestic Animals. In: Histological Classification of Tumors of the Alimentary System of Domestic Animals. Second Series. Washington, DC: Armed Forces Institute of Pathology.

Lee, N., Choi, M., Keh, S., Kim, T., Kim, H. and Yoon, J. 2014. Zygomatic sialolithiasis diagnosed with computed tomography in a dog. J. Vet. Med. Sci. 76, 1389-1391.

Li, J., Gong, X., Xiong, P., Xu, Q., Liu, Y., Chen, Y. and Tian, Z. 2014. Ultrasound and computed tomography features of primary acinic cell carcinoma in the parotid gland: A retrospective study. Eur. J. Radiol. 83, 1152-1156.

Liu, Y., Li, J., Tan, Y.R., Xiong, P. and Zhong, L.P. 2015. Accuracy of diagnosis of salivary gland tumors with the use of ultrasonography, computed tomography, and magnetic resonance imaging: A meta-analysis. Oral Surg. Oral Med. Oral Pathol. Oral Radiol. 119, 238-245.

Marconato, L. and Amadori, D. 2012. Oncologia medica veterinaria e comparata. Vermezzo: Poletto.

Militerno, G., Bazzo, R. and Marcato, P.S. 2005. Cytological diagnosis of mandibular salivary gland adenocarcinoma in a dog. J. Vet. Med. A Physiol. Pathol. Clin. Med. 52, 514-516.

Morris, J. and Dobson, J. 2001. Small Animal Oncology. Oxford: Blackwell Science Ltd. pp: 121-124.

Rastogi, R., Bhargava, S., Mallarajapatna, G.J. and Singh, S.K. 2012. Pictorial essay: Salivary gland imaging Indian J. Radiol. Imaging 22, 325-333.

Rudack, C., Jörg, S., Kloska, S., Stoll, W. and Thiede, O. 2007. Neither MRI, CT nor US is superior to diagnose tumors in the salivary glands--an extended case study. Head Face Med. 3, 19.

Sidaway, B.K., McLaughlin, R.M. and Hughes, J. 2004. Cervical masses in dogs: Diagnosis and treatment. Compend. Contin. Educ. Pract. Vet. 5, 390-402.

Smrkovski, O.A., LeBlanc, A.K., Smith, S.H., LeBlanc, C.J., Adams, W.H. and Tobias, K.M. 2006. Carcinoma ex pleomorphic adenoma with sebaceous differentiation in the mandibular salivary gland of a dog. Vet. Pathol. 43, 374-377.

Sozmen, M., Brown, P.J. and Eveson, J.W. 2003. Salivary gland basal cell adenocarcinoma: A report of cases in a cat and two dogs. J. Vet. Med. A Physiol. Pathol. Clin. Med. 50, 399-401.

Spangler, W.L. and Culbertson, M.R. 1991. Salivary gland disease in dogs and cats: 245 cases (1985–1988). J. Am. Vet. Med. Assoc. 198, 465-469.

Thackray, A.C. and Sobin, L.H. 1972. Histopathological typing of salivary gland tumours. In: World Health Organization, international histopathological classification of tumours. Geneva.

Torad, F.A. and Hassan, E.A. 2013. Clinical and ultrasonographic characteristics of salivary mucoceles in 13 dogs. Vet. Radiol. Ultrasound 54, 293-298.

Welkoborsky, H.J. 2011. Current aspects in ultrasonography of the salivary glands. HNO. 59, 155-165.

Yerli, H., Aydin, E., Coskun, M., Geyik, E., Ozluoglu, L.N., Haberal, N. and Kaskati, T. 2007. Dynamic multislice computed tomography findings for parotid gland tumors. J. Comput. Assist. Tomogr. 31, 309-316.